THE JOURNAL OF PHYSICAL CHEMISTRY A

Article

pubs.acs.org/JPCA

New Parameterization Scheme of DFT-D for Graphitic Materials

Karol Strutyński,[†] Manuel Melle-Franco,[†,‡] and José A. N. F. Gomes*[,†]

[†]REQUIMTE, Departamento de Química, Faculdade de Ciências, Universidade do Porto, Rua do Campo Alegre S/N, 4169-007 Porto, Portugal

[‡]Departamento de Informática, Centro de Ciências e Tecnologias da Computação, Universidade do Minho, 4710-057 Braga, Portugal

Supporting Information

ABSTRACT: A new parametrization scheme of DFT-D is proposed with the aim of devising a methodology for the study of graphitic material. The main feature of the new system is the geometry optimization within the fitting scheme. The DFT-D parameters are obtained for the benzene dimer, a good model molecule for graphitic systems. Very accurate CCSD(T) results are used as reference data for the benzene dimer, and the new method is shown to reproduce accurately its binding energies with small basis sets. After geometry optimization our new scheme performs better than the other methods. This approach generates proper geometries and accurate binding energies, even with small basis sets. We can expect this method to give similarly good results for larger graphitic systems.

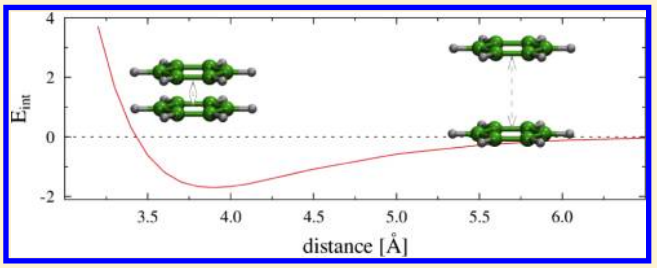

INTRODUCTION

Density functional theory (DFT) has become the method of choice for modeling complex systems in theoretical chemistry mainly due to its computational feasibility and the many functionals tailored for specific cases. However, in some situations currently available functionals fail to account for all physical interactions. Dispersion or van der Waals (vdW) interactions are a well-known failure within DFT. Local and semilocal exchange-correlation functionals do not give a proper description of electronic interactions in the region of low electron density, where vdW interactions play an important role. Advanced post-Hartree−Fock methods, like coupled cluster (CC) approaches, offer a very accurate description of dispersion forces. The problem is that CC, due to the very high computational costs, is only applicable for small systems and for a few points on their potential energy surface (PES);[1] moreover, huge basis sets are required for accurate results.

The inclusion of dispersion in density functional methods is an active field of research. Several routes are being explored, including electron-density-based approximations,[2,3] symmetry-adapted perturbation theory,[4] reparameterization of existing functionals,[5] use of effective core potentials,[6] or instantaneous dipole moment of the exchange hole.[7]

The most effective scheme to describe dispersion interactions is arguably that of adding a semiempirical dispersion term, the so-called DFT-D method.[8,9] This method has many advantages: Any functional can be augmented with an additional dispersion term, and it is easily incorporated into existing quantum mechanical programs, including the dispersion force gradients needed for geometry optimization. Furthermore DFT-D allows for an easy interpretation of the results as the dispersion energy may be partitioned into individual parts of a molecule or different distance ranges.

The aim of this work is to obtain a suitable method for studies of graphitic systems, especially van der Waals complexes and their energetics. Systems like graphite, fullerenes, or carbon nanotubes are very large, hence methods with low computational cost using small basis sets are to be preferred. Elusive van der Waals interactions play a very important role in both the energies and the geometries of those systems and have to be accurately described. The precise geometries of many graphitic systems are yet unknown, so any new method designed to produce accurate energies has to properly describe their geometries as well. We think that, after conveniently adjusting for graphitic systems, the DFT-D method will fulfill those requirements.

Benzene Dimer. The benzene dimer (BD) is arguably the smallest molecular analogue of graphitic materials. The study of aggregation of benzene molecules is difficult, both theoretically and experimentally, due to the weak binding.

Experimental data on the BD are scarce; the interaction energy is about −2.4 kcal/mol.[10] The exact geometry of the BD is not known, and the experiments showed that the minimum is most likely a T-shaped structure.[11]

In contrast, the benzene dimer has been the object of many theoretical studies yielding two almost isoenergetic minima (PD_a and TT_b) and, at least, eight stationary points.[4] The binding energy of the BD was theoretically found to be less than −3.0 kcal/mol.[1,12−14] The benzene dimer conformations presented in Figure 1 are used in this study.

Binding and Interaction Energy. For the aim of this paper, it is convenient to distinguish between binding and interaction energies. Figure 2 shows the energetics of the dimerization

Received: December 12, 2012
Revised: February 27, 2013
Published: March 8, 2013

 © 2013 American Chemical Society

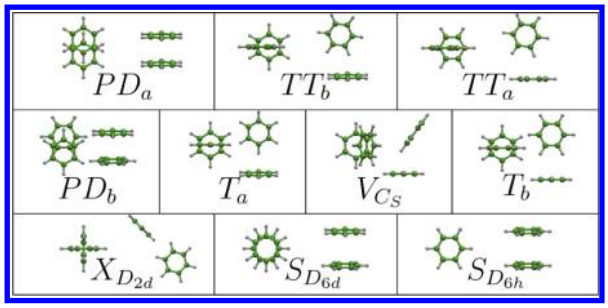

Figure 1. Benzene dimer structures: including parallel displaced (PD), sandwich type (S), T-shaped (T), tilted T-shaped (TT), V-shaped (V), and X-shaped (X) configurations. The subscript of the configuration indicates the symmetry of the molecule or the position of one molecule with respect to the other (a, over atom; b, over bond).

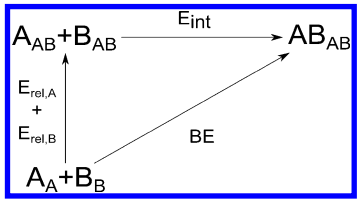

Figure 2. General dimerization process. Subscripts denote the geometry of the moiety.

process A + B → AB. In principle, a monomer in the dimer will deform, and its geometry in the dimer will be different from that in the separate moiety. The energy E_{rel} corresponds to the energy of that relaxation. The binding energy (BE) is the energy needed to separate the complex into two not interacting monomers (i.e., at infinite intermolecular distance)

$$\mathrm{BE} = E_{\mathrm{AB}_{\mathrm{AB}}} - E_{\mathrm{A}_{\mathrm{A}}} - E_{\mathrm{B}_{\mathrm{B}}} \tag{1}$$

where the subscripts denote the geometry of the molecule: AB_{AB} denotes the whole complex and B_B is the free monomer B.

In theoretical studies, it is common to use yet a different measure: the interaction energy defined as the energy difference between the complex and the monomers without relaxation

$$E_{\mathrm{int}} = E_{\mathrm{AB}_{\mathrm{AB}}} - E_{\mathrm{A}_{\mathrm{AB}}} - E_{\mathrm{B}_{\mathrm{AB}}} \tag{2}$$

This is a convenient definition, as one can use single-point (SP) energies of the monomers, without optimizing their geometries. As monomers do not usually deform in a significant manner, relaxation energy is small, and the E_{int} can be viewed as a first approximation of the more accurate binding energy.

The definitions presented above follow the intuitive notion that negative values correspond to bonded systems. This is the reason for not using the frequent convention, where both values are defined with a negative sign in eqs 1 and 2.

The terms interaction energy and binding energy are frequently used interchangeably in the literature. In most cases this does not present a problem when only one of the concepts is used. In this paper, we want to distinguish between those terms as the production of accurate geometries is one of the arguments of our study.

DFT-D METHODS

General Description. The DFT-D method augments the conventional DFT energy (E_{DFT}) with a damped London-type dispersion energy (E_{disp})

$$E_{DFT-D} = E_{DFT} + E_{disp} \tag{3}$$

The general form of the additional dispersion for a system with N_{at} atoms can be expressed as

$$E_{disp} = -\sum_{n} s_n \sum_{\substack{A,B \\ A>B}}^{N_{at}} \frac{C_{n,AB}}{R_{AB}^{n}} f_{dmp}(n, R_{AB}) \tag{4}$$

where n = 6, 8, 10, ... is the order of the expansion; $C_{n,AB}$ denotes the dispersion coefficient for an atom pair AB; and s_n is a global scaling factor for the dispersion. To avoid near singularities at small R_{AB} distances, the damping function f_{dmp} is introduced.

Most DFT-D methods truncate eq 4 at the first order, using only n = 6.

In principle this methodology of augmentation could be used to supplement other methods, e.g., HF, but only density functional methods will be considered here.

The most relevant implementations of this methodology are Grimme's DFT-D1,[15] DFT-D2,[16] and DFT-D3.[17]

The literature on the DFT-D method is extensive, and notations vary widely. Furthermore there are multiple approaches to obtain values of $C_{6,AB}$ coefficients and to compute the damping function f_{dmp}. A concise review of the most commonly used variations within the DFT-D method is given to fix the notation. After the review we will proceed to the description of the optimization procedure.

Dispersion Coefficients. An important part of the dispersion correction is the dispersion coefficients $C_{n,AB}$. Along with the s_n scaling factor, they control the strength of the interaction.

In the DFT-D1 implementation, the $C_{6,A}$ coefficients are empirical parameters, and the mixed value in the form of a harmonic mean is used.

The subsequent DFT-D2 method uses the geometric mean

$$C_{6,\mathrm{AB}} = \sqrt{C_{6,\mathrm{A}} C_{6,\mathrm{B}}} \tag{5}$$

with atomic values produced in a more ab initio manner: from the atoms' ionization potentials and their dipole polarizabilities: $C_{6,A} = 0.05 N I_{p,A} \alpha_A$.

Another mixing method often used is

$$C_{6,\mathrm{AB}} = 2\frac{(C_{6,\mathrm{A}}^2 N_{\mathrm{eff,A}} C_{6,\mathrm{B}}^2 N_{\mathrm{eff,B}})^{1/3}}{(C_{6,\mathrm{A}} N_{\mathrm{eff,B}}^2)^{1/3} + (C_{6,\mathrm{B}} N_{\mathrm{eff,A}}^2)^{1/3}} \tag{6}$$

where $N_{\mathrm{eff,A}}$ is the Slater–Kirkwood effective number of electrons.[13,18,19]

Damping Function. We should note that the correction in the $1/R^6$ form is only valid at large distances, and some medium-range correlation effects are already contained in the density functionals. At short distances standard functionals describe the systems rather well, and some damping function must be used to seamlessly merge the short-range functional with the long-range correction.

The damping function used in DFT-D1 and DFT-D2 methods is

$$f_{\mathrm{dmp}}(R_{\mathrm{AB}}) = \left\{1 + \exp\left[-\alpha\left(\frac{R_{\mathrm{AB}}}{r_{\mathrm{scl}} R_{\mathrm{AB}}^0} - 1\right)\right]\right\}^{-1} \tag{7}$$

It uses the parameters α controlling steepness and R_{AB}^0 to denote the cutoff distance. Usually R_{AB}^0 is some van der Waals radius. The scaling factor, r_{scl}, is introduced to properly describe the medium-range behavior of the DFT-D method, so it depends on the functional being used.

dx.doi.org/10.1021/jp312239n | J. Phys. Chem. A 2013, 117, 2844–2853

The newer DFT-D3 method could be used with two dampings: First, the zero-damping that vanishes in small distances, similarly to one used in the DFT-D1, The second approach, so-called Becke–Johnson damping, provides a constant and nonvanishing E_{disp} for short interatomic distances.

Various other damping methods were investigated,[8,20,21] and a universal damping function was proposed[22]

$$f_{dmp} = \left\{1 + a \exp\left[-b\left(\frac{R_{AB}}{r_{scl}R^0_{AB}}\right)^m\right]\right\}^n \quad (8)$$

where by adjusting a, b, m, and n parameters one can mimic other f_{dmp}.

Cutoff Radii. All damping functions use a cutoff radius R^0_{AB}. Mixed values are usually the sum of the atomic ones

$$R^0_{AB} = R^0_A + R^0_B \quad (9)$$

Another proposed mixing was[19]

$$R^0_{AB} = (R^{0^3}_A + R^{0^3}_B)/(R^{0^2}_A + R^{0^2}_B) \quad (10)$$

The DFT-D1 and DFT-D2 methods use for R^0_{AB} the radius corresponding to the 0.01 au electron density contour in a ROHF/TZV calculation. The DFT-D1 uses the radii scaling value of $r_{scl} = 1.22$, and the DFT-D2 decreased it to $r_{scl} = 1.10$.

DFT-D3. The newest approach of Grimme's group, the DFT-D3 method, is significantly different from the general methods presented above. A longer expansion including the $n = 8$ term is used (with $s_8 = 1$); there is an additional three-body term; and most parameters are obtained in a more ab initio manner.

Dispersion coefficients are obtained in a more elaborate process: First the $C_{n,AB}$ coefficients were obtained for various model molecules (e.g., A and B hydrides) and stored. Then, the values for $C_{6,AB}$ in the current molecule are computed from the stored data, including some information about the local geometry of the A and B atoms.

The DFT-D3 method takes another approach to obtain cutoff radii: R^0_{AB} is computed directly as the distance at which first-order AB interaction energy equals the cutoff energy. The cutoff energy was chosen to ensure the cutoff radii between carbon atoms to be the same as in the DFT-D2 method.

The DFT-D3 is an empirical method. The fact that most of the parameters are obtained in a systematic, more ab initio fashion, does not change that. It is possible to include more reference structures to obtain more reliable $C_{n,AB}$ coefficients,[23] but generally the DFT-D3 method is hard to adjust for specific systems.

The DFT-D1 and DFT-D2 methods are already available in many quantum mechanical programs. The older versions of the DFT-D3 are also present in some programs, but Grimme made the standalone program freely available, including the new parameter database.

Applicability of DFT-D. The benzene dimer was studied using DFT-D methods, and due to its small computational cost the method was even used for molecular dynamics.[24,25] Larger graphitic materials were also studied using the DFT-D approach.[26−29]

The DFT-D method was already fitted for the benzene dimer.[13,25] Pitoňák et al. performed a similar parametrization of DFT-D. Unfortunately, despite correspondence with the authors, we were unable to reproduce their E_{disp} values. Consequently we decided to parametrize the DFT-D2 method for the benzene dimer with an optimization scheme suited to our needs. The DFT-D2 method is already integrated into many quantum mechanical (QM) codes, and unlike DFT-D3, its parameters can be easily adjusted to allow for specific systems. The target systems are represented by similar structures, hence there is no great need for direct incorporation of the local chemical environment into dispersion, like in the DFT-D3 method. After preliminary testing we found that changing the mixing scheme does not introduce a significant difference, and we chose to modify the parameters with the default DFT-D2 mixing. Accordingly E_{disp} is computed using eqs 5, 7, and 9.

OPTIMIZATION PROCEDURE

Usually the DFT-D parameters are obtained by a process in which they are iteratively changed to best reproduce a set of reference energies. To make this process feasible for a large number of references, typically only single-point energy calculations are performed for the QM Hamiltonian (DFT functional and basis set) and for each reference conformation. This frozen geometry approach works well for a large number of reference molecules as many interatomic distances are sampled giving the proper energy dependence on the distance. When the number of reference structures is small it is more accurate to use relaxed optimization (Figure 3). In relaxed optimizations the geometries for each reference are optimized with the current DFT-D parameters.

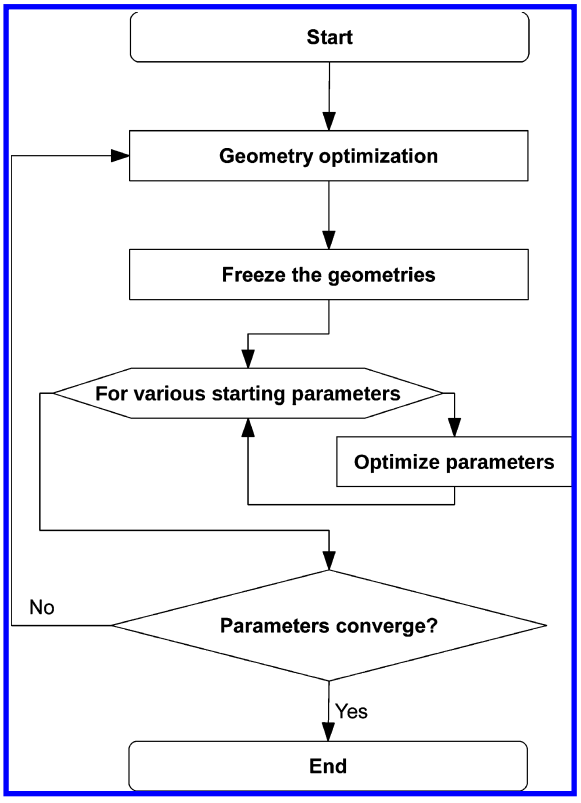

Figure 3. Relaxed fitting procedure flowchart.

As a reference for the optimization we have used the benzene dimer geometries presented in Figure 1, consisting of two minima and eight transition states. Their corresponding interaction energies were calculated as

$$E^{CCSD(T)}_{CBS} = E^{CCSD(T)}_{AVDZ} - E^{MP2}_{AVDZ} + E^{MP2}_{CBS} + E^{HF}_{AV5Z*} \quad (11)$$

dx.doi.org/10.1021/jp312239n | J. Phys. Chem. A 2013, 117, 2844−2853

where the correlation part of the interaction energy was extrapolated from SCS-MP2/AVTZ and SCS-MP2/AVQZ data along with HF/AV5Z* results to get the SCS-MP2/CBS limit. These, coupled cluster, energies were computed by Bludský et al.[14]

The root-mean-square difference of the binding energy (RMS(ΔBE)) from the DFT-D method with respect to the reference values was chosen as the function minimized in the optimization

$$\mathrm{RMS}(\Delta\mathrm{BE}) = \sqrt{\frac{1}{n_{\mathrm{sys}}}\sum_{i=1}^{n_{\mathrm{sys}}}(\Delta\mathrm{BE}_i)^2} \tag{12}$$

where $\Delta\mathrm{BE}_i = \mathrm{BE}_{i,\mathrm{CCSD(T)}} - \mathrm{BE}_{i,\mathrm{DFT\text{-}D}}$.

For the benzene dimer, at least three parameters ($C_{6,\mathrm{H}}$, $C_{6,\mathrm{C}}$, and r_{scl}) need normally to be optimized to perform a reasonable fitting. In the case of graphitic materials, carbon and hydrogen are the most abundant elements, and usually hydrogen plays a small role in vdW interactions, with the consequence that the impact of noncarbon elements on dispersion energy is small. For example, for the C_{60}−tetraphenylporphyrin complex all interactions with nitrogen are only 6% of E_{disp}, while C and H interactions account for 98 and 18%, respectively. For that reason we decided to use s_6 instead of the two C_6 coefficients, and the fact that only one DFT functional was used facilitates that optimization scheme.

Figure 3 presents our implementation of the relaxed fitting. In the initial step all geometries are optimized using the initial parameters (s_6 = 1.05, r_{scl} = 1.22). Then, these parameters are optimized using the Nelder−Mead method[30] to minimize the RMS(ΔBE) on the frozen geometries obtained in the last step. To avoid local minima, several fittings are performed from different starting points. In subsequent steps the geometry of all the molecules in the data set are progressively relaxed with new sets of parameters. The procedure is continued until convergence of the parameters or the RMS(ΔBE). Note that during geometry optimization some conformations may change. In principle some geometrical score function could be used to account for that, but for simplicity, we chose to monitor the geometries and discard parameters that cause conformation switching. The optimization scheme presented here will be referred to as Relaxed Fitting (RF).

The benzene dimer DFT-D calculations were performed using a modified version of NWChem 6.0 and NWChem 6.1.[31] Our modifications provide more control over the dispersion coefficients and allow for different mixing schemes. After preliminary testing, BLYP[32,33] was found to be one of the fastest and more accurate functionals, and it was chosen for parametrization. The Slater exchange[34] with Perdew 81 correlation[35] functional was used for a simple LDA comparison. The M05[5] and M06[36] families of functionals were chosen for comparison, and because of their numerical instability with the default grid, a bigger numerical grid was chosen (NWChem keyword "grid euler lebedev 96 11"). The zero-damping was used in all DFT-D3 calculations.

Parameters for BLYP-D with Pople's double-ζ, triple-ζ,[37,38] and Ahlrichs triple-ζ[39] basis sets with and without polarization were systematically obtained. For the Dunning−Hay SV and SVP basis sets[40] and the Ahlrichs DZ and DZP basis sets, optimizations were difficult, and good representations of all BD conformations were not achieved.

RESULTS AND DISCUSSION

Graphitic systems, of which very relevant examples are carbon nanotubes, fullerenes, and graphite, are systems that are locally similar to graphene. In such systems the parallel conformations of neighboring not connected rings are predominant. For this reason parallel BD conformations appear like a natural model to study those systems.

Two sets of benzene dimer conformations were chosen for the relaxed fitting described above: first, the set of four parallel structures ($\mathrm{PD_a}$, $\mathrm{PD_b}$, $S_{\mathrm{D_{6d}}}$, and $S_{\mathrm{D_{6h}}}$) and, second, the full set of all 10 conformations (see Figure 1). The optimization using the former set of structures was discarded, and its parameters will not be presented here, as we found that this parametrization model does not give a good representation of the other benzene dimer conformations. Moreover this optimization process may lead to nonphysical parameter values in some cases.

Three different values of the steepness of the damping function were used, $\alpha = \{6,15,20\}$, producing what we shall call RF-α sets of parameters for various basis sets. Table 1 presents the parameters obtained during the optimization process for α = 6 and α = 20. A damping function steepness of α = 15 shows some of the intermediate behavior between α = 6 and α = 20. Results for RF-15 will be presented in the Supporting Information only and will not be discussed here.

Table 1. Optimized RF Parameters for Various Basis Sets and the Corresponding Root Mean Square Errors of the Geometry Displacements (RMSD [Å]) and of the Benzene Dimer Binding Energy (RMS(ΔBE) [kcal/mol])[a]

basis	s_6	r_{scl}	α	RMSD	RMS(ΔBE)
6-31g	1.2100	1.3810	20	0.1022	0.2156
6-311g	1.4650	1.3810	20	0.1073	0.1538
TZV	1.3750	1.3060	20	0.0603	0.1221
TZVP	1.3790	1.2910	20	0.0511	0.1185
6-31g	**1.6190**	**1.4890**	**6**	**0.0858**	**0.2149**
6-311g	1.8110	1.4320	6	0.1245	0.1562
TZV	1.5320	1.2500	6	0.0367	0.1028
TZVP	**1.5130**	**1.2190**	**6**	**0.0334**	**0.0896**

[a]The recommended sets of parameters are in bold.

As expected, the energetic and geometrical errors decrease with growing basis sets. The geometrical errors are measured by the root-mean-square displacement (RMSD) of all atoms across all BD optimized conformations with respect to the reference structures. The RF-6 method with the relatively large TZVP basis set produces the best results. The final aim here is to use the resulting parameters in studies of graphitic systems. However, for larger systems, the use of the TZVP basis set is expensive and may not be feasible. For this reason we choose the set of parameters that not only results in the required accuracy but also is affordable with the available computational resources. For very large systems the RF-6/6-31G method appears as a reasonable compromise between accuracy and computational cost.

The next logical step is the comparison of the RF method with other methods designed for reproducing vdW interactions. This will show the reliability of the new method.

Comparison with Other Methods. The reference geometries, for comparison with the DFT-D method, were taken from Bludský et al.[14] Upon geometry optimization with different functionals and DFT-D methods, even the geometry of the

dx.doi.org/10.1021/jp312239n | J. Phys. Chem. A 2013, 117, 2844−2853

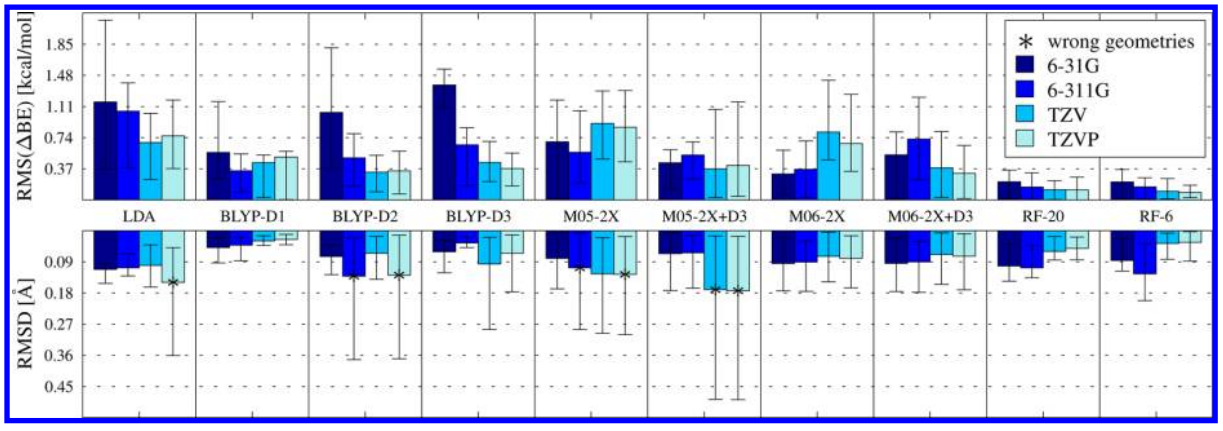

Figure 4. Binding energy errors (top) and geometrical differences (bottom) for the benzene dimer. Asterisks indicate that some conformations switch during geometry optimization. Error bars represent minimal and maximal |ΔBE| (top) or RMSD (down) among the benzene dimer conformations.

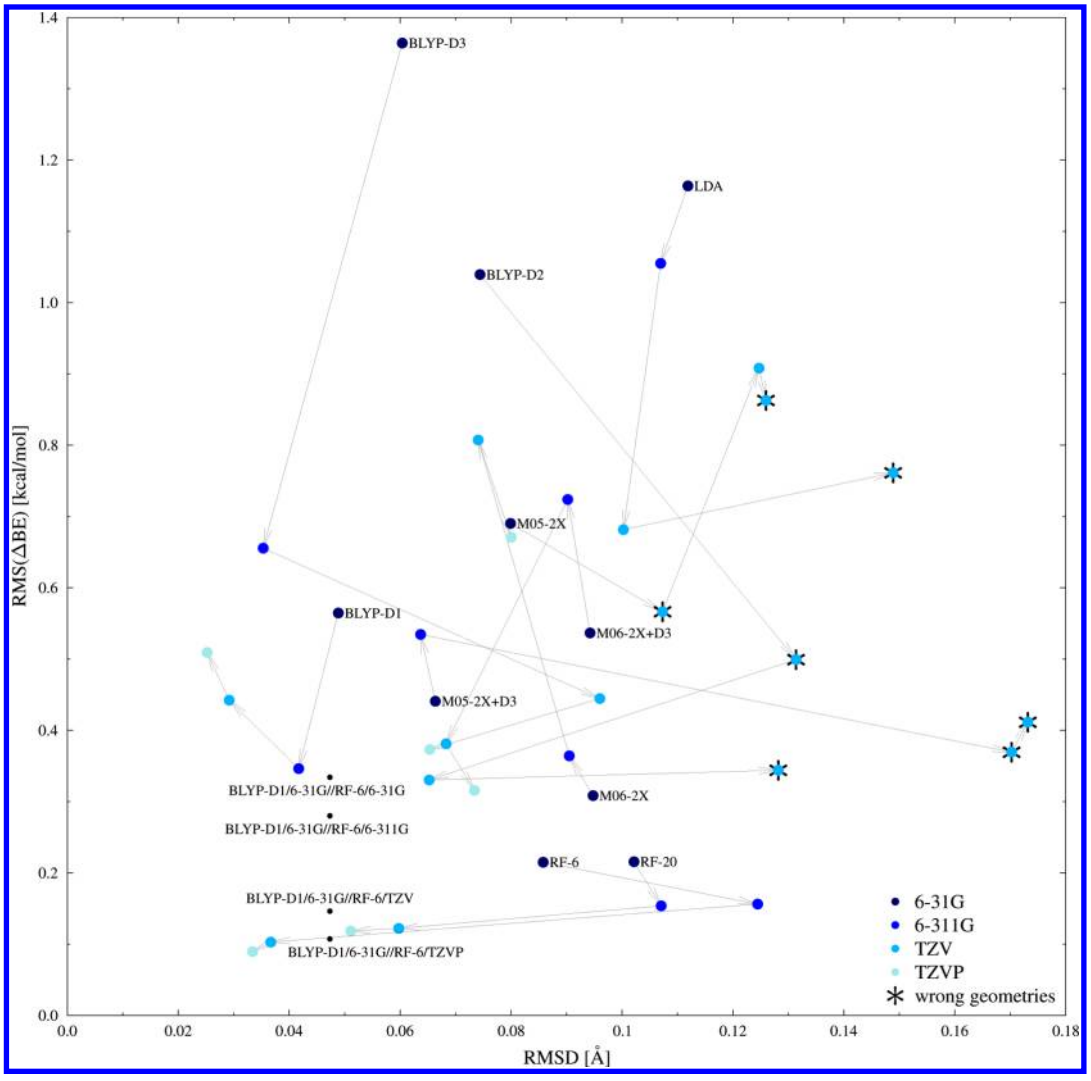

Figure 5. Binding energies and geometrical errors for the benzene dimer with different methods, *XY* plot. The RF methods provide very good results and ensure proper behavior with growing basis sets. The SP energy calculations using geometries obtained from the BLYP-D1/6-31G method are also shown as small black dots.

monomer changes slightly (RMSD of 0.001−0.021 Å) in comparison with the reference geometry.

Figures 4 and 5 present the root mean squares of the binding energy and geometrical differences after optimization of BD structures with different methods.

Figure 4 presents binding energies and geometrical errors of the investigated methods. Error bars show minimal and maximal discrepancies from the reference values among the BD conformations. It is important to note that RF methods provide precise results, this being confirmed by the very small gap

dx.doi.org/10.1021/jp312239n | J. Phys. Chem. A 2013, 117, 2844−2853

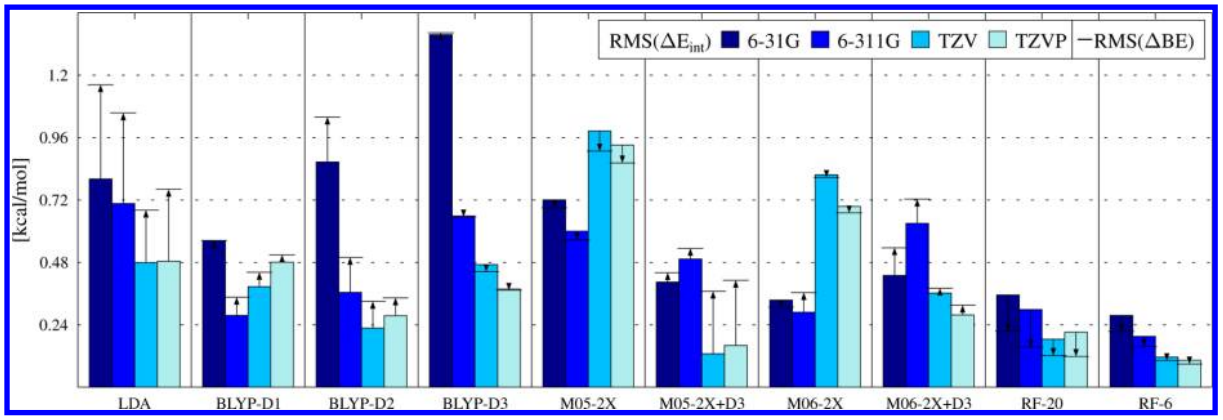

Figure 6. RMS differences between the calculated interaction and the binding energies of the benzene dimer and the reference values. The arrows point from the interaction energies (colored bars) to the binding energies for various methods. For binding energies, the new RF method gives better results than any other method, and especially small basis sets appear to be acceptable.

between the best and worst binding energies. Asterisks indicate that at least one conformation was not conserved during geometry optimization. Geometrical optimization using M05-2x-D3/TZV and M05-2x-D3/TZVP methods changed the $S_{D_{6d}}$ conformation into PD_b, but M05-2x without dispersion could reproduce it: the M05-2x/6-311G and M05-2x/TZVP have problems with V_{C_s} and PD_b conformations, respectively. The BLYP-D2 method causes switching V_{C_s} conformation into T_A.

In Figure 4, it is hard to compare the overall performance of the different methods. More informing is the *XY* plot of the binding energies and geometrical errors as presented in Figure 5. The results for each functional with growing basis set are connected with arrows. The methods with a bigger basis set should produce smaller geometrical differences and binding energies closer to the reference, CCSD(T)/CBS, data. Hence methods with growing basis sets should result in points closer to the origin of the plot. Only BLYP-D3 and RF methods behave as expected. However the BLYP-D3 method produces very large errors with small basis sets and could not be used with relatively large, graphitic systems. Surprisingly, the first generation of the Grimme, the BLYP-D1 method, gives very accurate geometries. The BLYP-D1 binding energies are comparable to other investigated methods. From Figure 5, it is clear that relaxed fitting methods perform very well. The RF geometrical errors are comparable to other methods, and the corresponding binding energies are superior.

To obtain the interaction energy, the previously known geometry of the complex is required or its geometry optimization must be performed. The E_{int} could be viewed as a first approximation of the true binding energy, which is more computationally demanding. Figure 6 shows the differences when one goes from E_{int}, at reference geometries, to BE, with complex and monomer relaxation.

Most methods considered here produce smaller errors without geometry optimization. This indicates that most methods were designed to reproduce single-point interaction energies and not true binding energies. The problem with that methodology arises when the structure of the systems is not known and the optimization of the geometry is required: methods that could not reproduce all BD conformations may produce inaccurate geometries. The RF method and the M05-2X functional perform consistently better using binding energies, but only the RF method provides satisfactory performance with growing basis sets, reproducing all BD conformations.

The standard procedure in theoretical studies is performing geometry optimization as a first step with a less accurate method, usually the same functional with a smaller basis set. A careful study of Figure 5 suggests that a good strategy for obtaining accurate binding energies at good geometries is to optimize the geometry of the system using BLYP-D1 with the 6-31G basis set and to get interaction energies from the RF method with a TZV or a TZVP basis set. The black point in Figure 5 represents results obtained using the RF-6 method on BLYP-D1/6-31G geometries. When one uses BLYP-D1/6-31G geometries for the SP calculation of the interaction energy with the RF-6/TZVP method, results are satisfactory: RMS(ΔE_{int}) = 0.11 kcal/mol with RMS for geometrical differences of 0.047 Å, at a fraction of the computational time for a TZVP geometry optimization (speedup of 5.6). For comparison, the results after geometry optimization at the RF-6/TZVP level are similar: RMS(ΔBE) = 0.09 kcal/mol and RMSD = 0.033 Å. The approach works well when large TZV or TZVP basis set are to be used to obtain the final energies.

Potential Energy Curve. The accurate representation of the geometry of the minima does not guarantee a good description of the van der Waals interaction, especially when the geometry of the system is optimized. During geometry optimization some steps may lead to conformations far from the geometry of the minima. The state of affairs is even worse when the geometry of the system is not known, as is the case with some graphitic materials. The appropriate method should describe the whole potential energy surface (PES) as accurately as possible.

At small intermolecular distances, where the molecules repel each other, the DFT functionals can properly describe the system. At medium-range distances, near the optimal geometry, DFT has problems with vdW complexes due to the inaccurate description of the electron correlation effects. However, most of the functionals investigated here behave properly as they were especially tailored for such systems. When the distance is large the electron density is low in the region between the monomers, but some van der Waals interactions are still present. The pure DFT description of the system fails to account for that. With growing intermolecular distance the interaction energy goes asymptotically to zero, so the dimer energy is equal to the sum of the energies of the free monomers. The potential energy scan can show the behavior of the given method at the mentioned intermolecular distances. The important part of the PES scan is between the minima and the long-range tail, because at those distances the pure DFT lacks a proper description. This region is

dx.doi.org/10.1021/jp312239n | J. Phys. Chem. A 2013, 117, 2844−2853

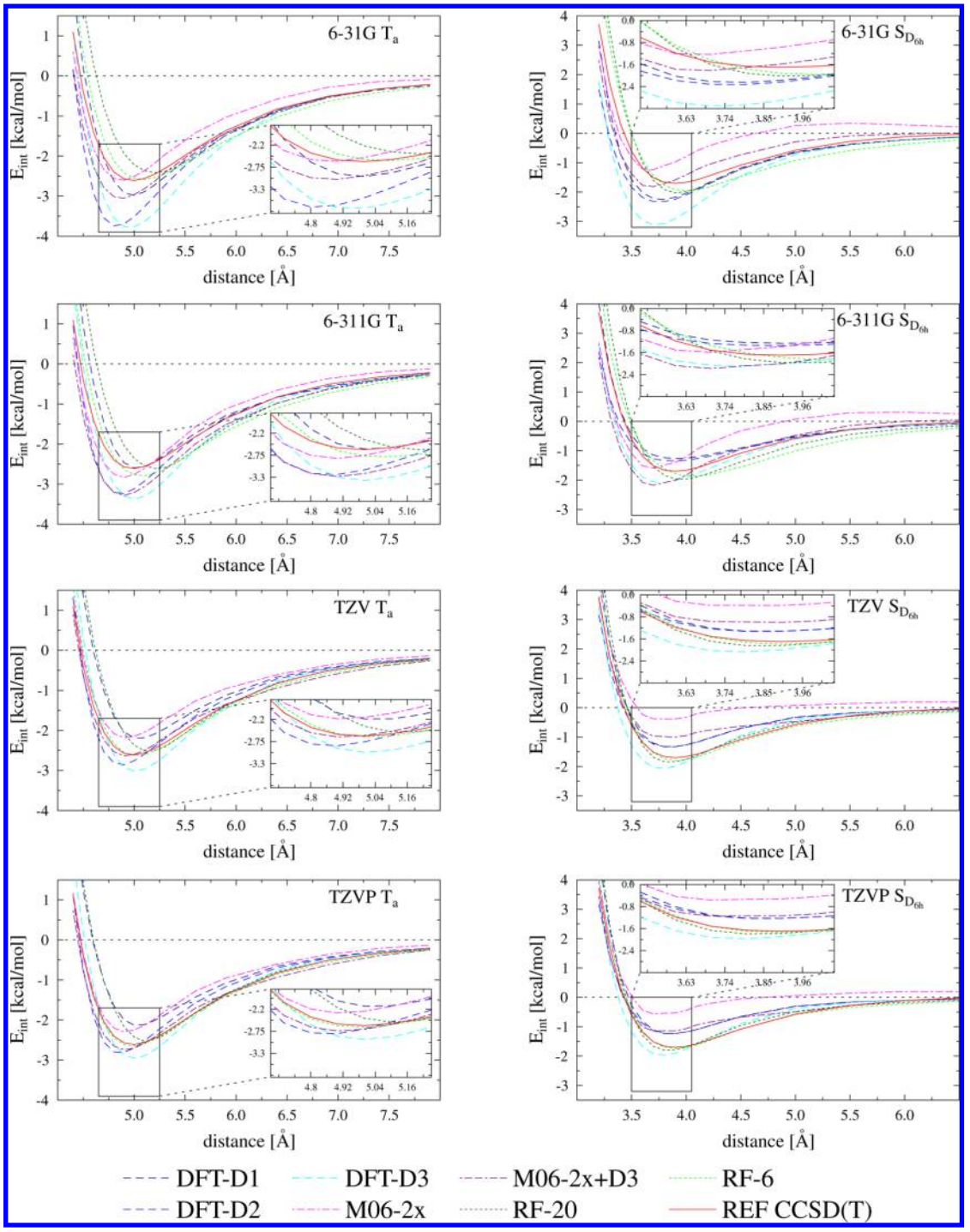

Figure 7. Potential energy curves for different functionals. The T_a (left) and $S_{D_{6h}}$ (right) benzene dimer conformations with various basis sets. Only the RF method behaves well with different basis set.

crucial for the description of the vdW bonded systems and shows how the additional dispersion connects noninteracting monomers, at large distances, with systems at short distances, that are well described by the DFT. The wrong description of this region of the PES could result in a shifted position of the minima and wrong interaction energies.

Figure 7 shows the evolution of the interaction energy with growing intermolecular distance for two conformations, $S_{D_{6h}}$ and T_a, with various basis sets. Figure 8 shows the evolution of the E_{int} for the PD_b dimer conformation at fixed separation between the benzene planes (at 3.6 and 3.8 Å) as the "sliding" displacement between the monomers changes.

As expected, the interaction energy for the M06-2X functional quickly declines as the intermolecular distance grows (see Figure 7). This shows how a simple reparameterization of the hybrid functional is insufficient to fully describe van der Waals interactions.

The general features of the PES are reproduced in all cases, but some important differences must be stressed. The position of the minimum, in Figure 7, depends markedly on the functional used but is less sensitive to the basis set. The same cannot be said

dx.doi.org/10.1021/jp312239n | J. Phys. Chem. A 2013, 117, 2844−2853

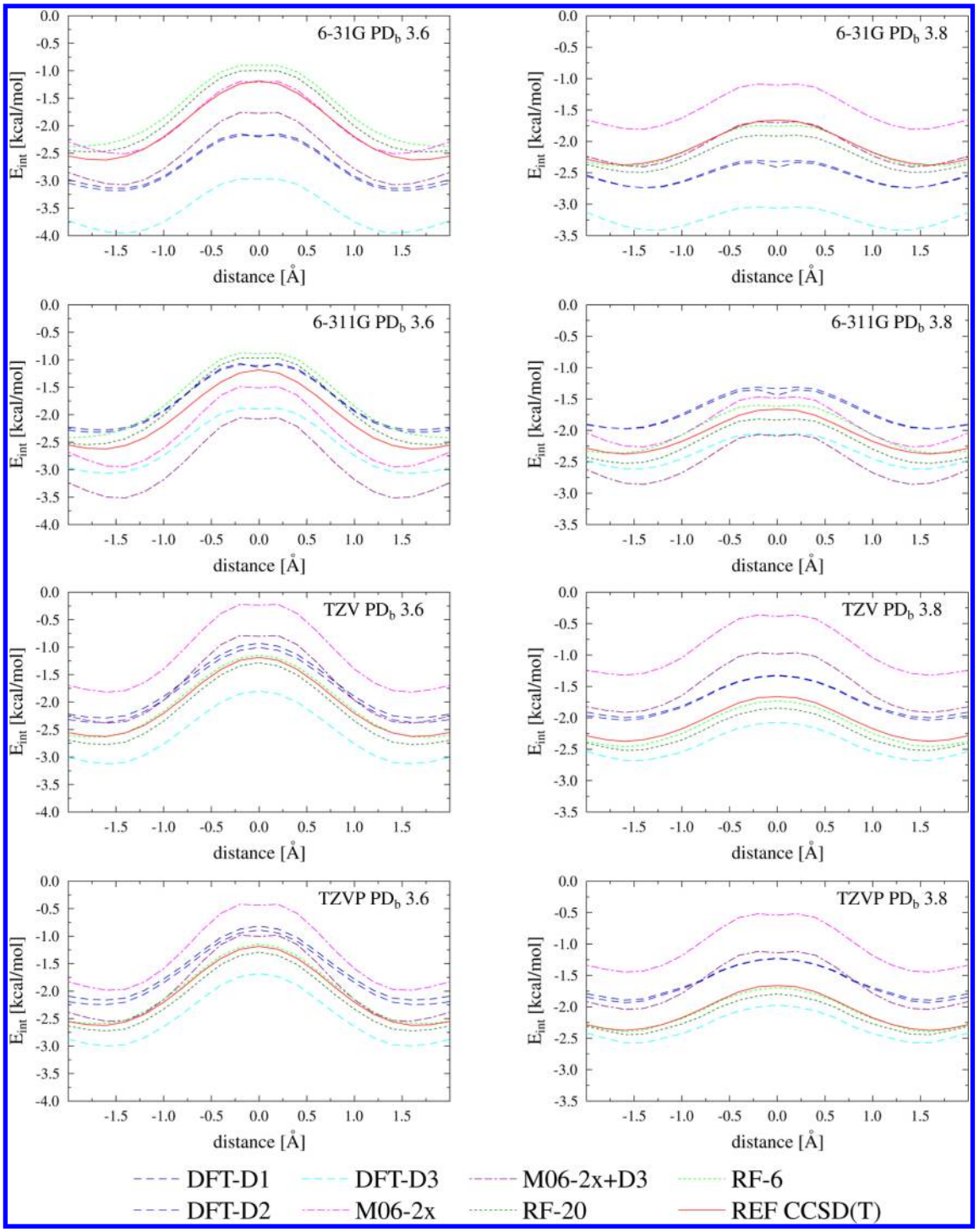

Figure 8. Potential energy curves for different functionals. Various displacements of monomers in PD$_b$ conformations at 3.6 and 3.8 Å separation.

about the energy of this equilibrium point, which shows important variations. The RF methods are the exception, as the position of the minimum is still almost unchanged, but the variations of the E_{int} are also small. The minimum position of the T_a conformation is more accurate with smaller steepness of $\alpha = 6$ in the RF-6 method. Furthermore, the use of larger basis sets with the RF-6 and RF-20 methods improves the reproduction of the rigorous CCSD(T)/CBS curve.

It is important to mention that these PES curves were not used as reference data during optimization. The fact that the RF method could reproduce so accurately the PES curves vouches for its reliability.

Large Graphitic Systems. To further validate the usability of the RF method, we tested it on larger graphitic systems, namely, graphite crystal and C_{60} fullerene. The binding energy of the graphite crystal is about twice that of two graphene layers, other values like exfoliation energy or cleavage energy also being used.[42] Usually the binding energy of two graphene layers is the reported value. The interlayer lattice constant (a_z, twice the interlayer distance) is known from experiment.[43]

dx.doi.org/10.1021/jp312239n | J. Phys. Chem. A 2013, 117, 2844−2853

The few experimental values available have been obtained indirectly with the fundamental aid of molecular mechanics simulations. The microscopy analysis of collapsed nanotubes by Benedict et al. yielded a -35^{+15}_{-10} meV/atom.[44] A higher value, -52^{+5}_{-5} meV/atom, was obtained from the desorption of polyaromatic hydrocarbons on graphite by Zacharia et al.[42]

The two most recent, and likely to be accurate, theoretical studies of graphite give more convergent results with binding energies of −56 and −48 meV/atom for quantum MonteCarlo and RPA-DFT, respectively.[45,46] Dispersion corrected DFT (B97-D2) has already been applied to the interaction of polyaromatic hydrocarbons of increasing sizes yielding the extrapolated binding energy of graphene of −66 meV/atom.[47]

We optimize the structure of the graphite crystal using the RF method. Figure 9 presents halved binding energies and errors of

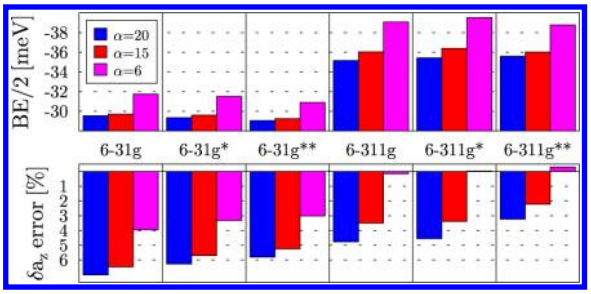

Figure 9. Half of the binding energy of graphite crystal (top) and error of the interlayer lattice constant (bottom).

the geometries obtained using the RF method for Pople's double- and triple-ζ basis sets. The best interlayer distances and largest binding energies are systematically obtained using the RF-6 method. The halved BE value (comparable to the BE of graphene) converges to about −40 meV/atom, which is well within the range of the mentioned literature data.

The structure of the C_{60} fullerene in the gas phase is known experimentally.[48] The RF-6/6311G method reproduces the bond lengths (1.46 and 1.40 Å) and the diameter (3.65 Å) of the molecule.

The fact that the RF method could accurately reproduce the features of the graphite and the C_{60} fullerene vouches for the transferability of the obtained parameters and confirms that the benzene dimer can be used as a model system for graphitic materials.

Basis Set Superposition. It is well-known that the QM calculated interaction energies do suffer from basis set superposition errors (BSSE), resulting in an apparently stronger bonding.

The most common technique of accounting for BSSE is the counterpoise (CP) correction by Boys and Bernardi that requires very demanding calculations of each interacting moiety using the basis set of the whole complex.[41] The methodology proposed in this paper aims at applications to relatively large systems, where CP correction would be practically unfeasible.

The dispersion correction proposed here was fitted to interaction energies that do not suffer from BSSE. If we were to go further and introduce a BSSE correction after our calculation, we would certainly underestimate the real interaction energies, as this correction introduces repulsive forces. To avoid this problem, the BSSE correction should be applied within the optimization procedure, but this would dramatically increase its computational cost. This is not to say that the BSSE is well represented by the dispersion correction adopted here but only that the results would deteriorate if the CP correction was to be introduced at the end. For simplicity of use and future application to large systems, we advise the use of RF methods without CP correction. The validity of that approach appears to be confirmed by the accurate reproduction of the reference energies that were achieved here by the RF method.

Computational Cost. The cost of the calculation of the E_{disp} correction is computationally negligible when compared with the quantum mechanical part of the calculation. Hence the computational cost of the DFT-D method is virtually identical to that of pure DFT (see Figure 10). The wall times for single-

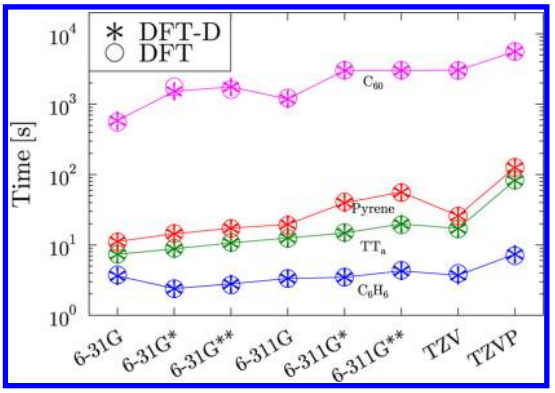

Figure 10. Log plot of wall times (average duration of each SCF cycle) for DFT and BLYP-D2 single-point calculations of benzene, benzene dimer, pyrene, and C_{60} fullerene for various basis sets. Using NWChem 6.1[31] on Intel(R) Core(TM)2 Quad CPU Q8400@2.66 GHz and 4 GB RAM.

point calculations of the C_{60} fullerene without symmetry with 6-31G and 6-311G basis sets are 4689 and 9478 s, respectively. The calculations were performed using an average current computer with Intel(R) Core(TM)2 Quad CPU Q8400@2.66 GHz processor and 4 GB RAM. This proves that the DFT-D method with double- or triple-ζ basis sets without polarization can perform calculations with up to ∼100 carbon atoms feasibly on current desktop computers. On supercomputers, computations are feasible for systems up to hundreds of carbons atoms.

CONCLUSIONS

The optimization scheme presented here allows the proposal of system-specific parameters for the DFT-D2 method. The main novelty is the geometry relaxation during optimization that allows the systems to adjust to current parameter values. The dispersion parameters for graphitic systems were obtained using the benzene dimer as a model system, resulting in the RF method.

The RF-6 method provides an accurate description of the weakly bonded benzene dimer with relatively small basis sets. The proper description of the van der Waals interaction is confirmed by the accurate reproduction of CCSD(T)/CBS potential energy curves.

Comparison with other methods shows that the geometry relaxation during optimization is crucial if accurate binding energies and reliable geometries are to be obtained. The accuracy of the interaction energy obtained without geometry optimization varies widely, but after optimization the RF method performs better than any other method, which shows the importance of relaxed fitting.

The RF-6 method did reproduce all known minima of the benzene dimer and scans of its potential energy surface, which

suggests that it will be able to accurately represent other graphitic systems, especially when precise geometries are unknown.

■ ASSOCIATED CONTENT

Supporting Information

The BLYP-D2 parameters obtained using relaxed optimization for all basis sets, the Cartesian coordinates and the binding energies at the CCSD(T)/CBS level of theory for all benzene dimer structures. This material is available free of charge via the Internet at http://pubs.acs.org.

■ AUTHOR INFORMATION

Corresponding Author

*E-mail: jfgomes@fc.up.pt.

Notes

The authors declare no competing financial interest.

■ ACKNOWLEDGMENTS

This work was supported by the Fundação para a Ciência e Tecnologia grant no. SFRH/BD/61894/2009.

■ REFERENCES

(1) Janowski, T.; Pulay, P. *Chem. Phys. Lett.* **2007**, *447*, 27−32.
(2) Dion, M.; Rydberg, H.; Schröder, E.; Langreth, D. C.; Lundqvist, B. I. *Phys. Rev. Lett.* **2004**, *92*, 246401.
(3) Becke, A. D.; Johnson, E. R. *J. Chem. Phys.* **2007**, *127*, 124108−124108−8.
(4) Podeszwa, R.; Bukowski, R.; Szalewicz, K. *J. Phys. Chem. A* **2006**, *110*, 10345−10354.
(5) Zhao, Y.; Truhlar, D. G. *J. Chem. Theory Comput.* **2007**, *3*, 289−300.
(6) von Lilienfeld, O. A.; Tavernelli, I.; Rothlisberger, U.; Sebastiani, D. *Phys. Rev. Lett.* **2004**, *93*, 153004.
(7) Johnson, E. R.; Becke, A. D. *J. Chem. Phys.* **2005**, *123*, 024101−024101−7.
(8) Elstner, M.; Hobza, P.; Frauenheim, T.; Suhai, S.; Kaxiras, E. *J. Chem. Phys.* **2001**, *114*, 5149−5155.
(9) Grimme, S. *Wiley Interdiscip. Rev.: Comput. Mol. Sci.* **2011**, *1*, 211−228.
(10) Grover, J. R.; Walters, E. A.; Hui, E. T. *J. Phys. Chem.* **1987**, *91*, 3233−3237.
(11) Arunan, E.; Gutowsky, H. S. *J. Chem. Phys.* **1993**, *98*, 4294−4296.
(12) Sinnokrot, M. O.; Sherrill, C. D. *J. Phys. Chem. A* **2004**, *108*, 10200−10207.
(13) Pitoňák, M.; Neogrády, P.; Řezáč, J.; Jurečka, P.; Urban, M.; Hobza, P. *J. Chem. Theory Comput.* **2008**, *4*, 1829−1834.
(14) Bludský, O.; Rubeš, M.; Soldán, P.; Nachtigall, P. *J. Chem. Phys.* **2008**, *128*, 114102.
(15) Grimme, S. *J. Comput. Chem.* **2004**, *25*, 1463−1473.
(16) Grimme, S. *J. Comput. Chem.* **2006**, *27*, 1787−1799.
(17) Grimme, S.; Antony, J.; Ehrlich, S.; Krieg, H. *J. Chem. Phys.* **2010**, *132*, 154104.
(18) Halgren, T. A. *J. Am. Chem. Soc.* **1992**, *114*, 7827−7843.
(19) Jurečka, P.; Černý, J.; Hobza, P.; Salahub, D. R. *J. Comput. Chem.* **2007**, *28*, 555−569.
(20) Ortmann, F.; Bechstedt, F.; Schmidt, W. G. *Phys. Rev. B* **2006**, *73*, 205101.
(21) Grimme, S.; Ehrlich, S.; Goerigk, L. *J. Comput. Chem.* **2011**, *32*, 1456−1465.
(22) Liu, Y.; Goddard, W. A. I. *Mater. Trans.* **2009**, *50*, 1664−1670.
(23) Ehrlich, S.; Moellmann, J.; Reckien, W.; Bredow, T.; Grimme, S. *ChemPhysChem* **2011**, *12*, 3414−3420.
(24) Pavone, M.; Rega, N.; Barone, V. *Chem. Phys. Lett.* **2008**, *452*, 333−339.
(25) Řezáč, J.; Hobza, P. *J. Chem. Theory Comput.* **2008**, *4*, 1835−1840.
(26) Voloshina, E.; Mollenhauer, D.; Chiappisi, L.; Paulus, B. *Chem. Phys. Lett.* **2011**, *510*, 220−223.
(27) Barone, V.; Casarin, M.; Forrer, D.; Pavone, M.; Sambi, M.; Vittadini, A. *J. Comput. Chem.* **2009**, *30*, 934−939.
(28) Valdés, H.; Klusák, V.; Pitoňák, M.; Exner, O.; Starý, I.; Hobza, P.; Rulíšek, L. *J. Comput. Chem.* **2008**, *29*, 861−870.
(29) Slstrokawinacuteska, J.; Dabrowski, P.; Zasada, I. *Phys. Rev. B* **2011**, *83*, 245429.
(30) Nelder, J. A.; Mead, R. *Comput. J.* **1965**, *7*, 308−313.
(31) Valiev, M.; Bylaska, E.; Govind, N.; Kowalski, K.; Straatsma, T.; Van Dam, H.; Wang, D.; Nieplocha, J.; Apra, E.; Windus, T.; de Jong, W. *Comput. Phys. Commun.* **2010**, *181*, 1477−1489.
(32) Becke, A. D. *Phys. Rev. A* **1988**, *38*, 3098−3100.
(33) Lee, C.; Yang, W.; Parr, R. G. *Phys. Rev. B* **1988**, *37*, 785−789.
(34) Slater, J. C.; Johnson, K. H. *Phys. Rev. B* **1972**, *5*, 844−853.
(35) Perdew, J. P.; Zunger, A. *Phys. Rev. B* **1981**, *23*, 5048−5079.
(36) Zhao, Y.; Truhlar, D. *Theor. Chim. Acta* **2008**, *120*, 215−241.
(37) Hehre, W. J. *J. Chem. Phys.* **1972**, *56*, 2257.
(38) Rassolov, V. A.; Pople, J. A.; Ratner, M. A.; Windus, T. L. *J. Chem. Phys.* **1998**, *109*, 1223.
(39) Schäfer, A.; Huber, C.; Ahlrichs, R. *J. Chem. Phys.* **1994**, *100*, 5829.
(40) Dunning, T. H. *J. Chem. Phys.* **1977**, *66*, 1382.
(41) Boys, S.; Bernardi, F. *Mol. Phys.* **1970**, *19*, 553−566.
(42) Zacharia, R.; Ulbricht, H.; Hertel, T. *Phys. Rev. B* **2004**, *69*, 155406.
(43) Baskin, Y.; Meyer, L. *Phys. Rev.* **1955**, *100*, 544.
(44) Benedict, L. X.; Chopra, N. G.; Cohen, M. L.; Zettl, A.; Louie, S. G.; Crespi, V. H. *Chem. Phys. Lett.* **1998**, *286*, 490−496.
(45) Spanu, L.; Sorella, S.; Galli, G. *Phys. Rev. Lett.* **2009**, *103*, 196401.
(46) Lebègue, S.; Harl, J.; Gould, T.; Ángyán, J. G.; Kresse, G.; Dobson, J. F. *Phys. Rev. Lett.* **2010**, *105*, 196401.
(47) Grimme, S.; Mück-Lichtenfeld, C.; Antony, J. *J. Phys. Chem. C* **2007**, *111*, 11199−11207.
(48) Hedberg, K.; Hedberg, L.; Bethune, D. S.; Brown, C. A.; Dorn, H. C.; Johnson, R. D.; Vries, M. D. *Science* **1991**, *254*, 410−412.